

Deep Generative Models for Library Augmentation in Multiple Endmember Spectral Mixture Analysis

Ricardo Augusto Borsoi, Tales Imbiriba, *Member, IEEE*, José Carlos Moreira Bermudez, *Senior Member, IEEE*,
Cédric Richard, *Senior Member, IEEE*

Abstract—Multiple Endmember Spectral Mixture Analysis (MESMA) is one of the leading approaches to perform spectral unmixing (SU) considering variability of the endmembers (EMs). It represents each endmember in the image using libraries of spectral signatures acquired *a priori*. However, existing spectral libraries are often small and unable to properly capture the variability of each endmember in practical scenes, what significantly compromises the performance of MESMA. In this paper, we propose a library augmentation strategy to improve the diversity of existing spectral libraries, thus improving their ability to represent the materials in real images. First, the proposed methodology leverages the power of deep generative models (DGMs) to learn the statistical distribution of the endmembers based on the spectral signatures available in the existing libraries. Afterwards, new samples can be drawn from the learned EM distributions and used to augment the spectral libraries, improving the overall quality of the unmixing process. Experimental results using synthetic and real data attest the superior performance of the proposed method even under library mismatch conditions.

Index Terms—Hyperspectral, endmember variability, spectral unmixing, generative models, MESMA, spectral libraries.

I. INTRODUCTION

Spectral Unmixing (SU) is part of a number of algorithms that retrieve vital information from hyperspectral images (HIs) in many applications [1]. SU aims at extracting the spectral signatures of materials present in the HI of a scene, which are called endmembers (EMs), as well as the proportion to which they contribute to each HI pixel. The SU problem can be solved using algorithms that are either supervised, where the EMs are known a priori, or unsupervised, where the EMs are estimated from the observed HI [2]. Different models have been proposed to describe the interaction between light and the targets [1], [3]. The most popular among these is the *Linear Mixing Model* (LMM), which represents the reflectance at each pixel as a convex combination of the spectral signatures of the endmembers. However, the LMM fails to represent important nonideal effects observed in many practical scenes, such as nonlinear interactions between light and the materials [3], [4], [5] and variations of the EM spectra along the scene [6].

EM variability is an important effect originating from environmental, illumination, atmospheric or temporal changes

which may lead to significant estimation errors throughout the unmixing process [7]. Different strategies have been proposed to deal with EM variability in SU. Although recent approaches include the use of statistical and parametric models to represent variable endmember spectra throughout the scene [7], [6], the most prominent approach, however, consists in considering EMs as sets of spectral signatures, also called spectral libraries [8]. In this case, the spectral signatures in each library are variants of a material produced under different acquisition conditions or physico-chemical compositions. They are usually acquired a priori through laboratory or *in situ* measurements. Under the LMM assumption, the unmixing problem then becomes equivalent to selecting a subset of signatures in the libraries that can best represent the observed HI. The methods that attempt to solve this problem can be roughly divided in two main categories: sparse unmixing [9], [10] and *Multiple Endmember Spectral Mixture Analysis* (MESMA) [11] algorithms. The MESMA algorithm is widely used due to its simplicity and interpretability, and has been employed in a large number of environments and scenarios [8, p.1607]. However, the quality of the MESMA or sparse SU results is strongly dependent on how well the available spectral libraries represent the endmember signatures actually present in the scene. This may cause a problem since spectral libraries are usually not acquired under the same conditions as the observed image, since *in situ* measurements can be costly or impractical. Furthermore, most existing spectral libraries only have very few signatures of each material, and might not adequately capture spectral variability occurring in the scene.

One approach to alleviate this problem consists of generating multiple synthetic samples of an endmember using a physical model (radiative transfer function - RTF) describing the variability of the spectra as a function of atmospheric or biophysical parameters [8], such as e.g. the PROSPECT of Hapke models [12], [13] for vegetation or mineral spectra. These additional signatures are then included in the library to augment it before performing SU. The use of RTFs to generate spectral libraries has great potential since it can represent spectral variability caused by different effects which are unlike to be captured by laboratory or field measurements [14], [15], [16]. However, physics-based models require accurate knowledge of the physical process governing the observation of the materials spectra by the sensor, which is hard to obtain in practice. This limits the practical interest of these methods.

Recently, deep generative models (DGMs) have seen remarkable advances in the form of variational autoencoders (VAEs) and generative adversarial networks (GANs) [17],

This work has been supported by the National Council for Scientific and Technological Development (CNPq).

R.A. Borsoi, T. Imbiriba and J.C.M. Bermudez are with the Federal University of Santa Catarina, Florianópolis, Brazil. e-mail: raborsoi@gmail.com; talesim@gmail.com; j.bermudez@ieee.org.

C. Richard is with the Université Côte d'Azur, Nice, France (e-mail: cedric.richard@unice.fr), Lagrange Laboratory (CNRS, OCA).

Manuscript received Month day, year; revised Month day, year.

[18]. These advances have made it possible to learn the distribution of complex (such as e.g. natural images) data very efficiently, and from a limited amount of samples [19]. DGMs have been considered for data augmentation in few-sample settings for image classification problems [19]. They have also been successfully used to represent the submanifold of EM spectra in blind unmixing applications [20].

In this paper, we propose a spectral library augmentation method for MESMA-based algorithms. Specifically, we propose to leverage the power of DGMs to augment the spectral libraries used to unmix the data with MESMA. The proposed strategy can be divided in three steps. First we learn the statistical distribution of each endmember in the scene using the spectral signatures contained in the existing spectral library and a generative model. Then, we sample new spectral signatures using the generative models and augment their respective spectral libraries. Finally, we unmix the observed HI using the MESMA algorithm and the augmented library. Simulations with synthetic and real data show a substantial accuracy gain in abundance estimation when comparing the proposed method with competing strategies.

This paper is organized as follows. The LMM and the MESMA algorithm are discussed in Section II. The proposed library augmentation strategy is presented in Section III. Simulations with synthetic and real data are presented in Section IV. Finally, concluding remarks are presented in Section V.

II. SPECTRAL UNMIXING WITH MESMA

Most MESMA algorithms consider the LMM as their central building block. The LMM assumes that each L -band pixel $\mathbf{y}_n \in \mathbb{R}^L$, $n = 1, \dots, N$, of a N -pixel HI, can be modeled as a convex combination of the spectral signatures of the endmembers in the scene:

$$\mathbf{y}_n = \mathbf{M}\mathbf{a}_n + \mathbf{e}_n, \text{ subject to } \mathbf{1}^\top \mathbf{a}_n = 1 \text{ and } \mathbf{a}_n \geq \mathbf{0} \quad (1)$$

where $\mathbf{M} \in \mathbb{R}^{L \times P}$ is a matrix whose columns are the P EM spectral signatures \mathbf{m}_k , \mathbf{a}_n is the abundance vector and \mathbf{e}_n is an additive noise term. Differently from most LMM-based HU methodologies, which assume a unique EM for each material in the scene, MESMA considers multiple spectra libraries, or bundles, one for each endmember, and performs a search for the best fitting model within all possible combinations of endmembers.

Thus, assuming prior knowledge of spectral bundles for each EM in the scene, the set \mathcal{M} of endmember matrices that can be drawn from the library can be defined as

$$\mathcal{M} = \left\{ [\mathbf{m}_1, \dots, \mathbf{m}_P] : \mathbf{m}_k \in \mathcal{M}_k, k = 1, \dots, P \right\} \quad (2)$$

where $\mathcal{M}_k = \{\mathbf{m}_{k,1}, \dots, \mathbf{m}_{k,C_k}\}$, $\mathbf{m}_{k,j} \in \mathbb{R}^L$ is a set of C_k spectral signatures of the k -th material. The MESMA SU problem can be formulated as

$$\begin{aligned} \min_{\mathbf{M} \in \mathcal{M}} \min_{\mathbf{a}_n} \|\mathbf{y}_n - \mathbf{M}\mathbf{a}_n\|_2^2 \\ \text{subject to } \mathbf{a}_n \geq \mathbf{0}, \mathbf{1}^\top \mathbf{a}_n = 1. \end{aligned} \quad (3)$$

Although the MESMA algorithm has shown excellent performance when dealing with spectral variability in many practical

scenarios, its performance is strongly effected by the quality of the spectral library \mathcal{M} [8]. In order for MESMA to perform well, the library must be representative of the spectral library observed in a given scene. Previous works tried to address this issue by augmenting the spectral libraries using physics-based models that describe well the variability of the endmembers. See, e.g., the PROSPECT or Hapke models [12], [13].

However, a major drawback of physics-based models is the requirement of accurate knowledge of the physical process governing the observation of the materials spectra by the sensor. This detailed information is rarely available in practice, which limits the applicability of these methods. In the following, we will present a new approach for spectral library augmentation that is based on deep generative models such as VAEs and GANs. These approaches allows one to learn the statistical distribution of the endmembers from very few training samples, making it effective in practical scenarios.

III. LIBRARY AUGMENTATION WITH GENERATIVE ENDMEMBER MODELS

Although physics-based models that accurately describe the variations of spectral library in a scene are often unavailable in practice, they reveal an important characteristic of spectral variability: that EM spectra usually lies on a low-dimensional submanifold of the high-dimensional spectral space \mathbb{R}^L . This assumption is in agreement with most physical models, such as the PROSPECT or Hapke models [12], [13], which represent the spectral signature of the materials as a function of only a small number of photometric or chemical properties.

Instead of employing physics-based models, we propose in this paper to augment the spectral libraries by using deep generative models. Generative models aim to estimate the probability distribution $p(X)$ of a random variable $X \in \mathbb{R}^L$ based on a set of N_x observations \mathbf{x}_i . Then, they allow one to generate new samples that look similar to new realizations of X . Such models have shown good performance at representing endmember spectra in blind unmixing applications [20]. Here we propose to use the signatures in existing spectral libraries to learn the generative models describing the distributions of EMs spectra. Then, to enhance the ability of the MESMA algorithm to adapt to a wider range of spectral variability, we augment the libraries by sampling from the estimated distributions. An illustrative outline of this strategy is shown in Fig. 1, with a VAE described in the following.

Even though the spectral dimensionality L is high compared to the small number of signatures often found in typical spectral libraries (which makes this problem very hard in general [21], [22]), the low-dimensionality of the manifolds to which the EM spectra is confined, allied with recent advances in generative models, have made this problem tractable. This framework has shown success in capturing the distribution of complex data such as natural images from extremely few training samples [19], which illustrates its appropriateness for our application. In the following we describe generative models, VAEs and GANs in particular, in more detail. Afterwards, we provide a detailed algorithm describing the proposed library augmentation procedure.

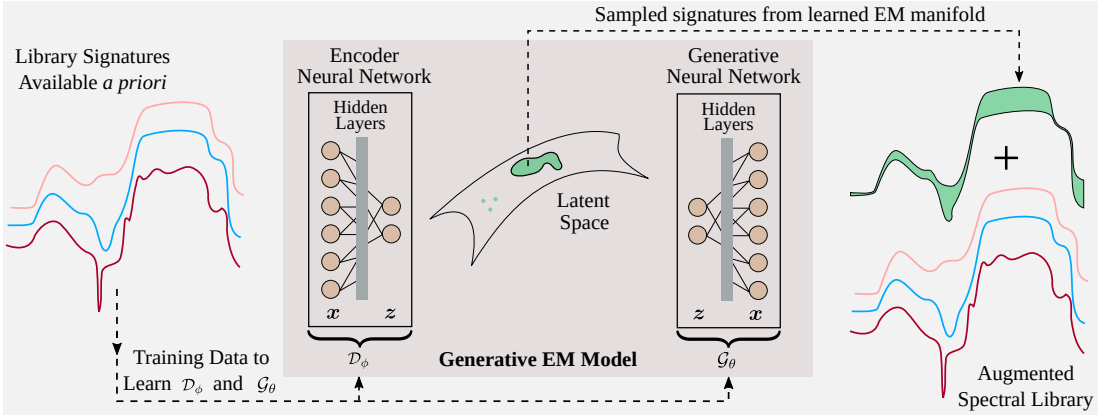


Figure 1. Outline of the proposed approach: deep generative models are used to approximate the distribution of spectra belonging to a library. Then, new spectral samples (right) can be obtained by propagating samples drawn from the EM submanifold through \mathcal{G}_θ and used to augment the spectral library.

A. Deep generative models

A convenient way to estimate the PDF $p(X)$ of a random variable X that lies on a low-dimensional submanifold of \mathbb{R}^L is to define a new random variable $\mathbb{R}^K \ni Z \sim p(Z)$, with $K \ll L$ and a known distribution $p(Z)$, and a parametric function (e.g. a neural network) \mathcal{G}_θ which maps $Z \mapsto \hat{X} \in \mathbb{R}^L$ such that the distribution of the transformed random variable $\hat{X} = \mathcal{G}_\theta(Z)$ is very close to $p(X)$. This allows us to generate new samples from \hat{X} by first sampling from $Z \sim p(Z)$ and then applying the function $\mathcal{G}_\theta(Z)$.

Although estimating \mathcal{G}_θ to fulfill this objective might seem difficult, recent advances in generative modeling such as VAEs [23] and GANs [18] have shown excellent performance for modeling complex distributions (e.g., of natural images) using only a limited amount of samples [19].

VAEs address this problem by maximizing a lower bound on the log-likelihood of $p(X)$ [23]:

$$\log p(X) \geq \mathbb{E}_{q_\phi(Z|X)} \{ \log p(X|Z) \} - KL(q_\phi(Z|X) \| p(Z))$$

where the function \mathcal{G}_θ is represented by $p(X|Z)$, $KL(\cdot \| \cdot)$ is the Kullback-Leibler divergence between two distributions, $\mathbb{E}_\zeta \{ \cdot \}$ is the expected value operator with respect to the distribution ζ and $q_\phi(Z|X)$ is a variational approximation to the intractable posterior $p(Z|X)$, which is also represented through another parametric function $\mathcal{D}_\phi : \mathbb{R}^L \rightarrow \mathbb{R}^K$.

Differently, GANs attempt to learn the distribution $p(X)$ by seeking for the Nash equilibrium of a two-player adversarial game [18] between the generator network \mathcal{G}_θ and a discriminator network \mathcal{C}_ϕ , which predicts the probability of a sample \mathbf{x}_i coming from the true distribution $p(X)$ instead of being generated through \mathcal{G}_θ . The generator \mathcal{G}_θ is trained to maximize the probability of the discriminator making a mistake, which is formulated as the following minimax optimization problem:

$$\min_{\mathcal{G}_\theta} \max_{\mathcal{C}_\phi} \mathbb{E}_{p(X)} \{ \log \mathcal{C}_\phi(X) \} + \mathbb{E}_{p(Z)} \{ (1 - \mathcal{C}_\phi(\mathcal{G}_\theta(Z))) \}.$$

Although GANs are more flexible and have shown better results when modeling complex distributions, they are also much harder to train [22]. This motivated us to use VAEs in this work due their more stable training procedure.

B. Library augmentation

Consider a small spectral library \mathcal{M} known a priori containing a set of spectral signatures \mathcal{M}_i for each material $i = 1, \dots, P$. Each signature $\mathbf{m}_{i,j} \in \mathcal{M}_i$, $j = 1, \dots, C_k$, can be viewed as a sample drawn from the statistical distribution of the i -th endmember spectra. Thus, these libraries can be employed as training data to learn a set of generative models \mathcal{G}_{θ_i} that represents the probability distribution function $p_i(M)$ of each endmember $i = 1, \dots, P$ using a VAE [23].

Given the learned generative models \mathcal{G}_{θ_i} , we can then generate new spectral signatures from each endmember class by sampling from the distribution of $\mathcal{G}_{\theta_i}(Z)$, where $Z \sim \mathcal{N}(0, \mathbf{I}_K)$. These new signatures can then be used to augment into the original library \mathcal{M} , yielding a new spectral library $\tilde{\mathcal{M}}$ which is more comprehensive and better accounts for different spectral variations of each material. Finally, the MESMA algorithm can be applied to unmix each image pixel \mathbf{y}_n using the augmented library $\tilde{\mathcal{M}}$. This procedure is described in detail in Algorithm 1, where the spectral library is augmented by adding N_s samples to each endmember set. Note that although this increases the complexity of SU with MESMA, approximate angle minimization-based strategies can be explored to obtain an efficient solution when the number of signatures in the augmented library (i.e. $C_k + N_s$) is large [24].

Algorithm 1: MESMA with spectral library augmentation

Input : \mathbf{Y} , \mathcal{M}_i , $i = 1, \dots, P$ and N_s .
Output: $\hat{\mathbf{A}}$ and $\tilde{\mathcal{M}}$.

- 1 **for** $i = 1, \dots, P$ **do**
- 2 Set $\tilde{\mathcal{M}}_i = \mathcal{M}_i$;
- 3 Train a deep generative model \mathcal{G}_{θ_i} using the samples in \mathcal{M}_i ;
- 4 **for** $j = 1, \dots, N_s$ **do**
- 5 Sample $\mathbf{z} \sim \mathcal{N}(0, \mathbf{I})$;
- 6 Compute $\tilde{\mathbf{m}} = \mathcal{G}_{\theta_i}(\mathbf{z})$;
- 7 $\tilde{\mathcal{M}}_i \leftarrow \mathcal{M}_i \cup \{ \tilde{\mathbf{m}} \}$;
- 8 **end**
- 9 **end**
- 10 Set $\tilde{\mathcal{M}} = \{ [\mathbf{m}_1, \dots, \mathbf{m}_P] : \mathbf{m}_k \in \tilde{\mathcal{M}}_k, k = 1, \dots, P \}$;
- 11 Run MESMA with the augmented library $\tilde{\mathcal{M}}$ to compute $\hat{\mathbf{A}}$;
- 12 **return** $\hat{\mathbf{A}}$, $\tilde{\mathcal{M}}$;

Table I
ENCODER AND DECODER NETWORK ARCHITECTURES.

	Layer	Activation	Number of units
\mathcal{D}_{ϕ}	Input	—	L
	Hidden # 1	ReLU	$\lceil 1.2 \times L \rceil + 5$
	Hidden # 2	ReLU	$\max \{ \lceil L/4 \rceil, K + 2 \} + 3$
	Hidden # 3	ReLU	$\max \{ \lceil L/10 \rceil, K + 1 \}$
\mathcal{G}_{θ}	Hidden # 1	ReLU	$\max \{ \lceil L/10 \rceil, K + 1 \}$
	Hidden # 2	ReLU	$\max \{ \lceil L/4 \rceil, K + 2 \} + 3$
	Hidden # 3	ReLU	$\lceil 1.2 \times L \rceil + 5$
	Output	Sigmoid	L

Table II
SIMULATIONS WITH SYNTHETIC AND REAL DATA (VALUES $\times 10^3$).

	Synthetic HI		Alunite Hill
	RMSE _A	RMSE _Y	RMSE _Y
FCLS	50.0 \pm 32.2	0.73 \pm 0.87	0.47 \pm 0.60
GLMM	45.3 \pm 31.2	0.30 \pm 0.22	10 ⁻⁶ \pm 2 \times 10 ⁻⁶
MESMA	18.2 \pm 13.7	0.41 \pm 0.45	19.2 \pm 14.0
Proposed	15.3 \pm 11.0	0.26 \pm 0.25	18.4 \pm 12.8

C. Network architecture

To learn the generative models \mathcal{G}_{θ_p} , we used a VAE [23] due to its stable training [22] and because it behaved well with small spectral libraries. The network architectures for \mathcal{G}_{θ_p} and \mathcal{D}_{ϕ_p} and the dimension of the latent spaces were selected as in [20] since they resulted in a good experimental performance and showed sufficient capacity to capture the spectral variability of a given library. The network architectures are shown in Table I and the latent spaces dimension was set to $K = 2$. Finally, the network training was performed with the Adam optimizer [17] in TensorFlow for 50 epochs.

IV. EXPERIMENTAL RESULTS

In this section, simulation results using both synthetic and real data illustrate the performance of the proposed method. We compare the performance of MESMA using the augmented library with that of the traditional MESMA algorithm. For a better comparison, we also present results obtained with the fully constrained least squares (FCLS) and the the GLMM [6], which estimate the endmembers from the observed HI (without using a spectral library). In all experiments, the VCA algorithm [25] was used to extract the reference EM matrix \mathcal{M}_0 from the observed HI and to initialize the FCLS and GLMM methods. The performances were evaluated using the Root Means Squared Error (RMSE) between the estimated abundance maps (RMSE_A) and between the reconstructed images (RMSE_Y). The RMSE between two generic matrices is defined as

$$\text{RMSE}_{\mathcal{X}} = \sqrt{\frac{1}{N_{\mathcal{X}}} \|\mathcal{X} - \mathcal{X}^*\|_F^2} \quad (4)$$

where $N_{\mathcal{X}}$ denotes the number of elements in the matrix \mathcal{X} .

A. Synthetic data with library mismatch

In this example, we evaluate the performance of the proposed approach quantitatively using a synthetic data set with three endmembers and $L = 198$ spectral bands. The goal is

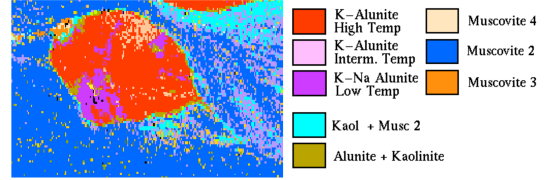


Figure 2. Alunite Hill classification maps released by USGS.

to simulate a typical library mismatch scenario often found when considering library-based unmixing [9]. To generate and process this dataset, we first obtained two disjoint sets of endmember spectra \mathcal{M}_i^1 and \mathcal{M}_i^2 , with $\mathcal{M}_i^1 \cap \mathcal{M}_i^2 = \emptyset$, $i \in \{1, 2, 3\}$ by manually extracting pure pixels of soil, vegetation and water from a real hyperspectral scene (the Jasper Ridge HI [26]). The sets \mathcal{M}_i^1 were used to compose the synthetic pixel spectra \mathbf{y}_n , and the sets \mathcal{M}_i^2 were used to perform unmixing with the MESMA algorithm. We simulated a library mismatch by applying a random affine transformation (a gain and an additive scaling in the intervals $[0.75, 1.25]$ and $[-0.15, 0.15]$, respectively) to each element of \mathcal{M}_i^2 , $i \in \{1, 2, 3\}$.

To generate each pixel, we used the LMM considering abundance fractions \mathbf{a}_n sampled from a flat Dirichlet distribution and pixel-dependent endmember matrices obtained by randomly (uniformly) selecting one spectral signature from each of the sets \mathcal{M}_i^1 , $i \in \{1, 2, 3\}$. WGN with an SNR of 30dB was added to the data.

The final library \mathcal{M} available for the MESMA-based methods was created by sampling three signatures at random of each material from \mathcal{M}_i^2 , and no other preprocessing or adequacy strategy was used to mitigate mismatch between the available library and the true endmembers used to construct the scene. Finally, in order to provide a proper statistical evaluation, this whole procedure was repeated for 10⁴ Monte Carlo realizations. The mean values and standard deviations are shown in Table II.

It can be seen that the proposed strategy provided a substantial (16%) improvement in the abundance estimation RMSE when compared to the MESMA algorithm. When compared with the other methods the proposed solution improvement is even more significant obtaining gains of 70% (FCLS) and 67% (GLMM). These experiments show that the proposed data augmentation strategy can lead to significant performance gains when compared to the plain MESMA algorithm.

B. Real data

For the simulation with real data, we considered the Alunite Hill subsene of the Cuprite dataset, containing three dominant endmembers (alunite, kaolinite and muscovite). This scene, with 28 by 16 pixels, was captured by the AVIRIS instrument, and water absorption or low SNR bands were removed, yielding $L = 181$ spectral bands. This region was selected since the distribution of materials therein has been released by USGS in the form of a high-resolution classification map (shown in Fig. 2), which can be used to evaluate the unmixing results. To build the library \mathcal{M} , we selected two signatures of each endmember from the USGS library such that the MESMA results best approached (visually) the ground truth.

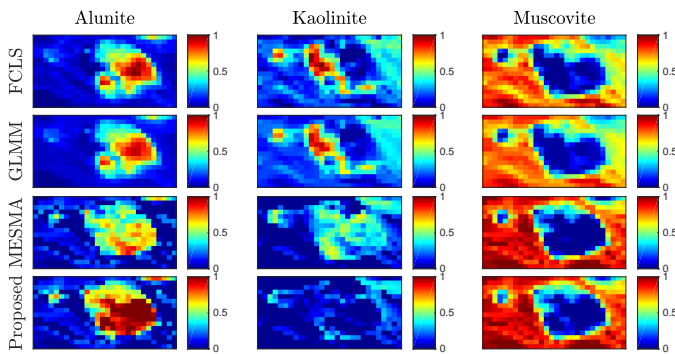


Figure 3. Abundance maps for the Alunite Hill subscene.

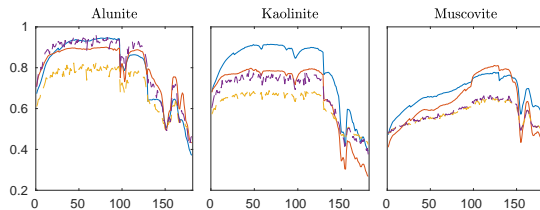


Figure 4. Original endmembers (solid line) and synthetically generated signatures (dashed line).

The abundance maps reconstructed by all algorithms are provided in Fig. 3. It can be seen that the abundance maps of the MESMA-based methods are significantly closer to the ground truth when compared to the GLMM and FCLS results. Furthermore, the proposed library augmentation strategy led to a much better representation of the alunite and kaolinite endmembers when compared to the competing approaches. The spectral signatures generated using the DGMs, shown in Fig. 4, show that the proposed strategy is able to generate signatures that accommodate variability seen in typical scenes, with a generally agreeable shape but different scaling variations that act nonuniformly over the spectral space.

V. CONCLUSIONS

In this work, a novel spectral library augmentation strategy was proposed for MESMA-like algorithms. Using the spectral signatures present in existing libraries as training samples, we applied deep generative models to learn the statistical distribution of endmember spectra. This allowed us to sample new spectral signatures from the estimated endmember distribution, which were then included in the augmented library, improving its ability to properly represent the materials present in practical scenes. Simulation results with both synthetic and real data showed that the proposed methodology can significantly improve the performance of the MESMA algorithm.

REFERENCES

- [1] N. Keshava and J. F. Mustard, "Spectral unmixing," *IEEE Signal Processing Magazine*, vol. 19, no. 1, pp. 44–57, 2002.
- [2] R. Ammanouil, A. Ferrari, C. Richard, and D. Mary, "Blind and fully constrained unmixing of hyperspectral images," *Image Processing, IEEE Transactions on*, vol. 23, no. 12, pp. 5510–5518, 2014.
- [3] N. Dobigeon, J.-Y. Tourneret, C. Richard, J. C. M. Bermudez, S. McLaughlin, and A. O. Hero, "Nonlinear unmixing of hyperspectral images: Models and algorithms," *IEEE Signal Processing Magazine*, vol. 31, no. 1, pp. 82–94, Jan 2014.
- [4] T. Imbiriba, J. C. M. Bermudez, C. Richard, and J.-Y. Tourneret, "Nonparametric detection of nonlinearly mixed pixels and endmember estimation in hyperspectral images," *IEEE Transactions on Image Processing*, vol. 25, no. 3, pp. 1136–1151, March 2016.
- [5] T. Imbiriba, J. C. M. Bermudez, and C. Richard, "Band selection for nonlinear unmixing of hyperspectral images as a maximal clique problem," *IEEE Transactions on Image Processing*, vol. 26, no. 5, pp. 2179–2191, May 2017.
- [6] T. Imbiriba, R. A. Borsoi, and J. C. M. Bermudez, "Generalized linear mixing model accounting for endmember variability," in *2018 IEEE International Conference on Acoustics, Speech and Signal Processing (ICASSP)*. IEEE, 2018, pp. 1862–1866.
- [7] A. Zare and K. C. Ho, "Endmember variability in hyperspectral analysis: Addressing spectral variability during spectral unmixing," *Signal Processing Magazine, IEEE*, vol. 31, pp. 95–104, January 2014.
- [8] B. Somers, G. P. Asner, L. Tits, and P. Coppin, "Endmember variability in spectral mixture analysis: A review," *Remote Sensing of Environment*, vol. 115, no. 7, pp. 1603–1616, 2011.
- [9] M.-D. Iordache, J. M. Bioucas-Dias, and A. Plaza, "Total variation spatial regularization for sparse hyperspectral unmixing," *IEEE Transactions on Geoscience and Remote Sensing*, vol. 50, no. 11, pp. 4484–4502, 2012.
- [10] R. A. Borsoi, T. Imbiriba, J. C. M. Bermudez, and C. Richard, "A fast multiscale spatial regularization for sparse hyperspectral unmixing," *IEEE Geoscience and Remote Sensing Letters*, vol. 16, no. 4, pp. 598–602, April 2019.
- [11] D. A. Roberts, M. Gardner, R. Church, S. Ustin, G. Scheer, and R. Green, "Mapping chaparral in the santa monica mountains using multiple endmember spectral mixture models," *Remote Sensing of Environment*, vol. 65, no. 3, pp. 267–279, 1998.
- [12] S. Jacquemoud and F. Baret, "PROSPECT: A model of leaf optical properties spectra," *Remote sensing of environment*, vol. 34, no. 2, pp. 75–91, 1990.
- [13] B. Hapke, "Bidirectional reflectance spectroscopy, 1, Theory," *Journal of Geophysical Research*, vol. 86, no. B4, pp. 3039–3054, 1981.
- [14] D. R. Peddle, F. G. Hall, and E. F. LeDrew, "Spectral mixture analysis and geometric-optical reflectance modeling of boreal forest biophysical structure," *Remote Sensing of Environment*, vol. 67, no. 3, pp. 288–297, 1999.
- [15] P. E. Dennison, K. Charoensiri, D. A. Roberts, S. H. Peterson, and R. O. Green, "Wildfire temperature and land cover modeling using hyperspectral data," *Remote Sensing of Environment*, vol. 100, no. 2, pp. 212–222, 2006.
- [16] B. Somers, S. Delalieux, W. W. Verstraeten, and P. Coppin, "A conceptual framework for the simultaneous extraction of sub-pixel spatial extent and spectral characteristics of crops," *Photogrammetric Engineering & Remote Sensing*, vol. 75, no. 1, pp. 57–68, 2009.
- [17] D. P. Kingma and J. Ba, "Adam: A method for stochastic optimization," in *International Conference on Learning Representations (ICLR)*, 2015. [Online]. Available: <https://arxiv.org/pdf/1412.6980.pdf>
- [18] I. Goodfellow, J. Pouget-Abadie, M. Mirza, B. Xu, D. Warde-Farley, S. Ozair, A. Courville, and Y. Bengio, "Generative adversarial nets," in *Advances in neural information processing systems*, 2014, pp. 2672–2680.
- [19] A. Antoniou, A. Storkey, and H. Edwards, "Data augmentation generative adversarial networks," *arXiv preprint arXiv:1711.04340*, 2017.
- [20] R. A. Borsoi, T. Imbiriba, and J. C. M. Bermudez, "Deep generative end-member modeling: An application to unsupervised spectral unmixing," *IEEE Transactions on Computational Imaging (accepted)*, 2019.
- [21] R. M. Neal, "Annealed importance sampling," *Statistics and computing*, vol. 11, no. 2, pp. 125–139, 2001.
- [22] M. Arjovsky, S. Chintala, and L. Bottou, "Wasserstein generative adversarial networks," in *International Conference on Machine Learning*, 2017, pp. 214–223.
- [23] D. P. Kingma and M. Welling, "Auto-encoding variational bayes," in *Proceedings of the International Conference on Learning Representations (ICLR)*, 2014. [Online]. Available: <https://arxiv.org/pdf/1312.6114.pdf>
- [24] R. Heylen, A. Zare, P. Gader, and P. Scheunders, "Hyperspectral unmixing with endmember variability via alternating angle minimization," *IEEE Transactions on Geoscience and Remote Sensing*, vol. 54, no. 8, pp. 4983–4993, 2016.
- [25] J. M. P. Nascimento and J. M. Bioucas-Dias, "Vertex Component Analysis: A fast algorithm to unmix hyperspectral data," *IEEE Transactions on Geoscience and Remote Sensing*, vol. 43, no. 4, pp. 898–910, April 2005.
- [26] T. Imbiriba, R. A. Borsoi, and J. C. M. Bermudez, "Low-rank tensor modeling for hyperspectral unmixing accounting for spectral variability," *arXiv preprint arXiv:1811.02413*, 2018.